# EDGC: Entropy-driven Dynamic Gradient Compression for Efficient LLM Training

Qingao Yi<sup>1</sup>, Jiaang Duan<sup>2</sup>, Hanwen Hu<sup>2</sup>, Qin Hua<sup>2</sup>, Haiyan Zhao<sup>1</sup>, Shiyou Qian<sup>2</sup>, Dingyu Yang<sup>3</sup> Jian Cao<sup>2</sup>, Jinghua Tang<sup>2</sup>, Yinghao Yu<sup>4</sup>, Chenzhi Liao<sup>4</sup>, Kangjin Wang<sup>4</sup>, and Liping Zhang<sup>4</sup>

<sup>1</sup>University of Shanghai for Science and Technology, Shanghai, China

<sup>2</sup>Shanghai Jiao Tong University, Shanghai, China

<sup>3</sup>Zhejiang University, Hangzhou, China

<sup>4</sup>Alibaba Group, Hangzhou, China

Abstract—Training large language models (LLMs) poses significant challenges regarding computational resources and memory capacity. Although distributed training techniques help mitigate these issues, they still suffer from considerable communication overhead. Existing approaches primarily rely on static gradient compression to enhance communication efficiency; however, these methods neglect the dynamic nature of evolving gradients during training, leading to performance degradation. Accelerating LLM training via compression without sacrificing performance remains a challenge. In this paper, we propose an entropy-driven dynamic gradient compression framework called EDGC. The core concept is to adjust the compression rate during LLM training based on the evolving trends of gradient entropy, taking into account both compression efficiency and error. EDGC consists of three key components. First, it employs a down-sampling method to efficiently estimate gradient entropy, reducing computation overhead. Second, it establishes a theoretical model linking compression rate with gradient entropy, enabling more informed compression decisions. Lastly, a window-based adjustment mechanism dynamically adapts the compression rate across pipeline stages, improving communication efficiency and maintaining model performance. We implemented EDGC on a 32-NVIDIA-V100 cluster and a 64-NVIDIA-H100 cluster to train GPT2-2.5B and GPT2-12.1B, respectively. The results show that EDGC significantly reduces communication latency and training time by up to 46.45% and 16.13% while preserving LLM accuracy.

#### I. Introduction

LLMs, such as GPT-4 [47] and Llama-3 [14], significantly influence areas like personal assistants [21], code programming [18], and search engines [33] with remarkable effectiveness. However, these advancements also bring substantial challenges. The scale of LLMs is growing exponentially [30], [65], making their training both computationally intensive and time-consuming. The computational power of individual GPUs is increasingly unable to keep up with the growth of LLMs [48]. To address this challenge, various distributed training strategies have been proposed [13].

Common parallel strategies include data parallelism (DP) [9], [26], [35], pipeline parallelism (PP) [30], [44], [45], tensor parallelism (TP) [36], [68], [71], Zero Redundancy Optimizer (ZeRO) [52], context parallelism (CP) [14], expert parallelism (EP) [12], [28], [57], and hybrid parallelism [34], [43], [46]. For instance, 3D parallelism effectively combines data, pipeline, and tensor parallelism to tackle the challenges of training LLMs. While 3D parallelism offers notable benefits

in memory efficiency and training performance, its complex communication requirements can increase bandwidth and latency demands, posing significant challenges.

Several methods have been proposed to reduce communication overhead, including modifying communication topologies [23], applying gradient compression [7], [38], optimizing synchronization [6], [42], [50], and overlapping computation with communication [59], [60]. Notably, gradient compression effectively decreases the data exchanged during training, which reduces bandwidth demands and accelerates convergence. Recent advancements in system architectures, such as DeepSpeed [53] and Megatron-LM [61], aim to lower memory and communication overheads through various mechanisms. DeepSpeed partitions optimizer states, gradients, and model parameters across multiple devices, while Megatron-LM optimizes communication using different parallelism strategies. Optimus-CC [62] enhances these advantages by compressing both data parallelism and pipeline (inter-stage) communication.

However, existing compression methods have two main limitations. (1) Most adopt fixed-rate strategies that fail to adapt to the dynamic nature of gradient updates, leading to suboptimal trade-offs between communication cost and model accuracy. (2) Compression rates are often determined empirically due to the absence of theoretical guidance, resulting in time-consuming and inefficient tuning processes. Furthermore, communication demands and bottlenecks can vary across pipeline stages during training, posing additional challenges for compression strategies.

By conducting evaluations on widely used LLMs, we identify three characteristics of their gradients: decreasing entropy, increasing zero-centralization, and matrix correlation (§III). First, in line with loss convergence, gradient entropy gradually decreases during training, indicating the potential for adjusting the compression rate. Second, the range of gradient variation iteratively narrows, trending toward zero-centralization, which suggests effectiveness for low-rank decomposition [31], [66]. Third, the correlations among LLMs' gradients ensure that the actual compression error from low-rank decomposition is lower than the theoretical error.

Based on these insights, we propose EDGC, an entropydriven dynamic gradient compression framework (§IV). Uti-

TABLE I: Parallelization strategies of different models

Organization	Model	Parallel Strategies
Google DeepMind	Gemini [54]	DP + PP + TP + EP
Meta	LLaMA3 [14]	DP + PP + TP + CP
DeepSeek AI	DeepSeek [39]	PP + DP + EP
Google Research	Switch Transformer [17]	DP + PP + TP + EP
EleutherAI	GPT-NeoX [4]	DP + PP + TP

lizing the low-rank decomposition as the compression engine, EDGC dynamically adjusts compression rates by leveraging the evolution of gradient entropy while maintaining LLM performance. Firstly, EDGC employs a sampling method to capture variations in gradient entropy, addressing the challenge of managing extensive gradient data. Secondly, we establish a theoretical model that quantifies the relationship between gradient entropy and compression rank, providing a foundation for dynamically adjusting the compression rate based on entropy fluctuations and compression error. Finally, EDGC adjusts compression using a window mechanism, determining appropriate compression rates and communication times for different iterations and pipeline stages.

We implemented EDGC in two setups (§V): a 32×NVIDIA V100 cluster with 32Gbps bandwidth for GPT2-2.5B and a 64×NVIDIA H100 cluster with 400Gbps bandwidth for GPT2-12.1B. We compared EDGC to three baselines: no-compression Megatron-LM [61], fixed-rank PowerSGD [66], and Optimus-CC [62]. The results show that EDGC significantly reduces communication time while maintaining model accuracy. Specifically, EDGC achieves up to 46.45% reduction in communication latency and 16.1% training time savings on GPT2-12.1B, and 45.8% and 14.64% on GPT2-2.5B, respectively. These results demonstrate the effectiveness of EDGC, surpassing static and stage-selective strategies across various LLM scales.

In summary, our contributions can be outlined as follows:

- Theoretically, we establish a theoretical model that defines the relationship between gradient entropy and compression rank, serving as a foundation for EDGC design.
- Methodologically, we design and implement EDGC for efficient LLM training, aiming to effectively reduce communication data while maintaining model accuracy.
- Experimentally, we assess EDGC using the GPT2-2.5B and GPT2-12.1B models across various cluster environments and network bandwidths to evaluate its performance.

The remainder of this paper is structured as follows: Section III introduces the background knowledge; Section III presents our observations; Section IV details the design of EDGC; Section V analyzes the experimental results; Section VI discusses key aspects of EDGC; Sections VII reviews related work; and VIII concludes the paper.

#### II. BACKGROUND

## A. Parallel Training Strategies

Table I summarizes the parallel strategies of several prominent LLMs. It shows that most mainstream LLMs adopt a hybrid parallelism approach, integrating data, pipeline, and

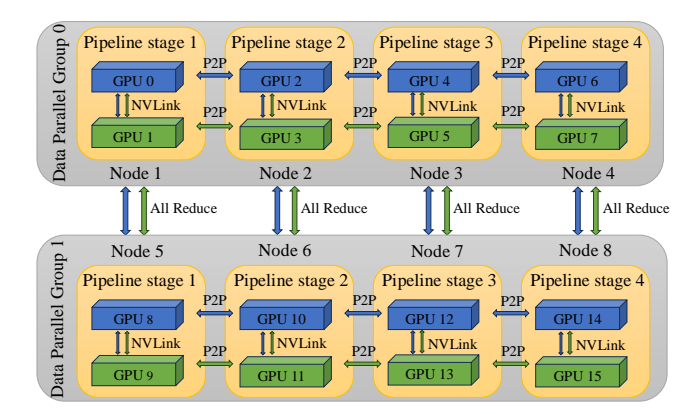


Fig. 1: An example topology of a 3D parallelism paradigm

tensor parallelism -commonly known as 3D parallelism. This strategy allows LLM training to scale efficiently across tens of thousands of GPUs, enabling the training of trillion-scale models. By integrating various parallelism techniques, 3D parallelism enhances memory and computational efficiency. It strategically allocates computing units to optimize each method. For instance, tensor parallelism, which incurs high communication costs, is confined to a single node to leverage the higher intra-node bandwidth (e.g., NVLink). Conversely, pipeline and data parallelism, with lower communication costs, are better suited for inter-node scheduling.

Figure 1 illustrates a 3D parallelism paradigm with a cluster of 8 nodes, each containing 2 GPUs. To implement 3D parallelism effectively, we set TP to 2, allowing GPUs within each node to leverage NVLink's high bandwidth. PP is configured to 4, necessitating that the number of layers in the LLM be divisible by this size for load balance and computational efficiency. DP is set to 2 to enhance GPU utilization, which focuses on parameter synchronization.

#### B. Low-rank Decomposition

Low-rank decomposition compresses gradients by approximating them as products of smaller matrices [27], [72]. For instance, Singular Value Decomposition expresses a matrix as the product of three matrices, with the singular value matrix at the center. PowerSGD [66] uses power iteration and orthogonalization to derive low-rank matrices that closely approximate the original gradients. The compression rank refers to the size of the factor matrices used to reconstruct the gradient. A smaller rank implies a higher compression rate and lower communication overhead.

#### III. OBSERVATIONS AND INSIGHTS

We analyze gradient evolution patterns during LLM training to inform EDGC design. We pre-trained GPT2-345M [51] and BERT [11] using the OpenWebText [24] and Wikipedia [19] datasets, respectively. The experiments employed an 8-node setup, with each node equipped two NVIDIA Tesla V100-SXM2 GPUs, each having 32GB memory. Each node also includes 16 CPU cores and 128GB RAM. Node communication occurs over 32Gbps Ethernet, while intra-node communication is facilitated by 300Gbps NVLink.

#### A. Observations

Training an LLM requires ongoing gradient computation and the update of billions of weights. These weights create a dynamic system that transitions from disorder to order. Initially, they are randomly initialized, leading to high uncertainty characterized by high entropy. As training progresses and weights undergo multiple gradient updates, they stabilize, leading to gradients conveying similar information. The evolution of LLM gradients reveals three key characteristics: a decrease in gradient information entropy, zero-centralization of gradients, and correlation among gradients.

Observation 1: The information entropy of gradients transitions from an unstable to a dynamically stable state during LLM training.

**Definition 1: Entropy of Continuous Random Variable.** For a continuous random variable X with probability density function f(x), the information entropy is defined as H(X), i.e.,

$$H(X) = -\int_{-\infty}^{\infty} f(x) \log f(x) dx \tag{1}$$

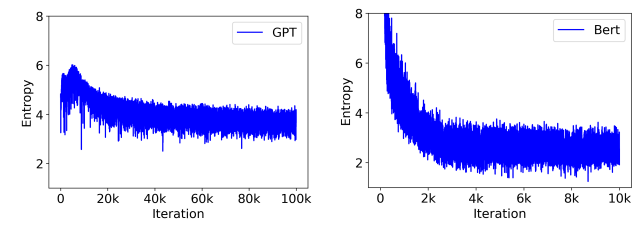
Entropy H(X) quantifies the uncertainty associated with the outcomes of the random variable X. Higher values indicate greater uncertainty.

Entropy reflects the uncertainty associated with gradient information during model training. We analyze the evolution of gradient entropy for GPT2-345M and BERT across training iterations, as shown in Figure 2. Both models display similar trends: an initial phase of instability marked by high entropy values, followed by a stabilization phase where entropy gradually decreases and converges. However, they exhibit distinct patterns of entropy change in two dimensions.

First, the duration of instability in LLMs varies significantly. For example, GPT and BERT achieve stability around iteration 100,000 and 10,000, respectively. This underscores the need for tailored compression strategies: BERT can be compressed more rapidly due to its earlier stability, while GPT necessitates a slower, more cautious approach. Second, entropy fluctuations exhibit varying magnitudes during the convergence process. For GPT, the entropy remains stable within a narrow range of 3.3–4.3, while BERT's entropy shows slightly greater variability at 1.8-3.8. This suggests that GPT's gradients converge more consistently, whereas BERT's gradients exhibit some variability. Consequently, more precise adjustments to compression rates are necessary for different LLMs to ensure stability.

# Observation 2: As iterations progress, the gradient variation range narrows, indicating a trend toward centralization.

We examine the gradient evolution patterns of GPT2-345M across randomly selected layers (0, 6, 12, and 18) at various times (0, 4k, 8k, 12k, and 16k iterations), as illustrated in Figure 3. Our findings indicate a convergence trend in gradient distribution among layers as training advances. Initially, a broad gradient distribution suggests significant uncertainty in capturing data features; however, with increasing iterations, model stability improves, as evidenced by the convergence



(a) Entropy changes in GPT2-345M

(b) Entropy changes in Bert

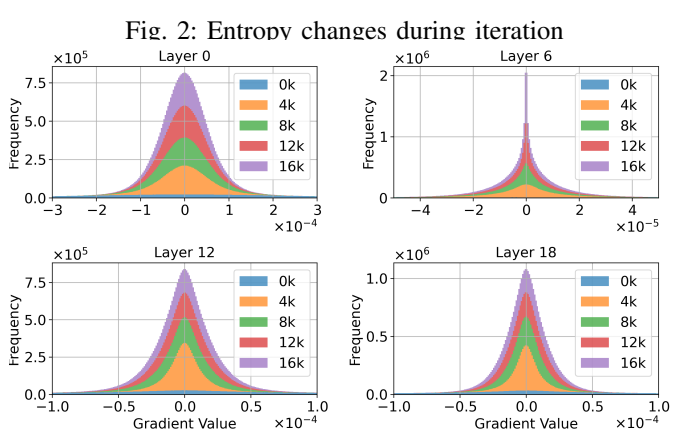


Fig. 3: Gradient distribution of GPT2-345M across different model layers at different iterations

of gradients. The reduction in gradient range reflects the model's ongoing refinement in feature learning and adaptation, highlighting a centralization in information processing.

Gradient convergence patterns are closely related to the dynamic adjustment of the learning rate in model training. A higher learning rate at the beginning allows for larger gradient updates, enabling the model to converge quickly and find a suitable parameter direction. As training progresses, the learning rate gradually decreases, especially with the widely used cosine annealing strategy [40]. This approach begins with a slow reduction in the learning rate, followed by a more rapid decline to a lower value, which reduces the volatility of gradient updates.

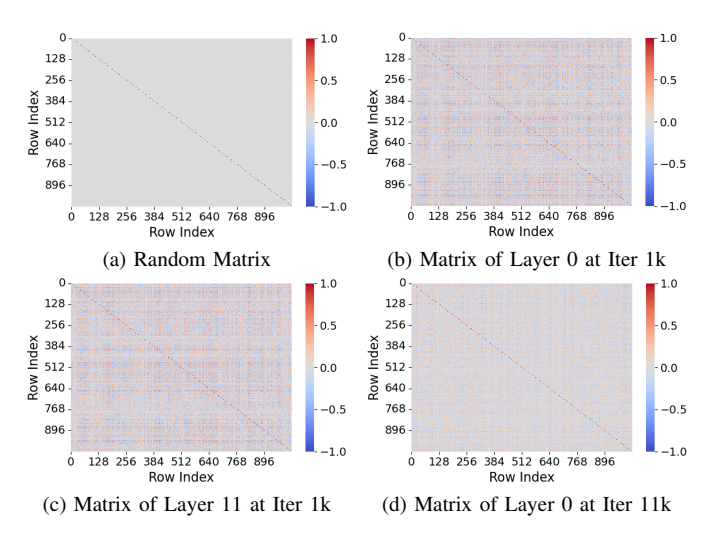


Fig. 4: Gradient matrix correlation of GPT-2

# Observation 3: During the training process, there are correlations between the LLM's gradient matrices.

During the iterative training of neural networks, we observed significant correlations among the gradient matrices of different parameters. These correlations arise from two primary sources: (1) Backpropagation mechanism: The gradient calculation inherently depends on the chain rule, leading to structural correlations among gradients. (2) Parameter coupling: The process of updating model parameters alters the network's behavior, causing subsequent gradient calculations to rely on the current state of the parameters, which introduces dynamic correlations.

To analyze these phenomena, we pre-trained GPT2-345M and collected gradient data from each layer at different iterations. We visualized the correlation heatmaps of the gradient matrices using the Pearson correlation coefficient. Figure 4a shows the gradient correlation heatmap generated from random data. The matrix shows no correlation, serving as a baseline reference for data analysis. In the early stages of training (e.g., at 1k iterations), gradient matrices exhibit strong correlations, as shown in the heatmaps for layer 0 and 11 (Figure 4b and 4c). This indicates that parameter adjustments in the early stages are structured and synergistic, likely driven by the backpropagation mechanism and initial parameter coupling. However, as training advances (e.g., at 11k iterations), the correlation among gradients decreases significantly, as shown by the heatmap for layer 0 in Figure 4d. This suggests that as the model approaches a stable state, the dynamic interactions between parameters weaken, leading to reduced gradient correlations.

# B. Insights

As highlighted in Observation 2, many gradients cluster near zero, suggesting that gradient quantization may lead to excessive zeroing and substantial information loss [20], [77]. Additionally, top-k sparsification methods may significantly impact model accuracy [62]. In contrast, low-rank decomposition effectively minimizes inter-node communication overhead while ensuring strong performance. Based on these findings, we implement low-rank decomposition for gradient compression, helping to reduce the risk of information loss from quantization.

Several methods employ low-rank approximation [66], [67], [73] and error feedback mechanisms [32], [56] to improve inter-node communication. However, these methods often overlook the dynamic nature of gradient changes. Our findings reveal a gradual decrease in gradient entropy, indicating loss convergence during training. By leveraging this trend, we introduce EDGC to dynamically modify compression ranks across various iterations and pipeline stages. EDGC seeks to minimize communication overhead while maintaining the performance of LLMs.

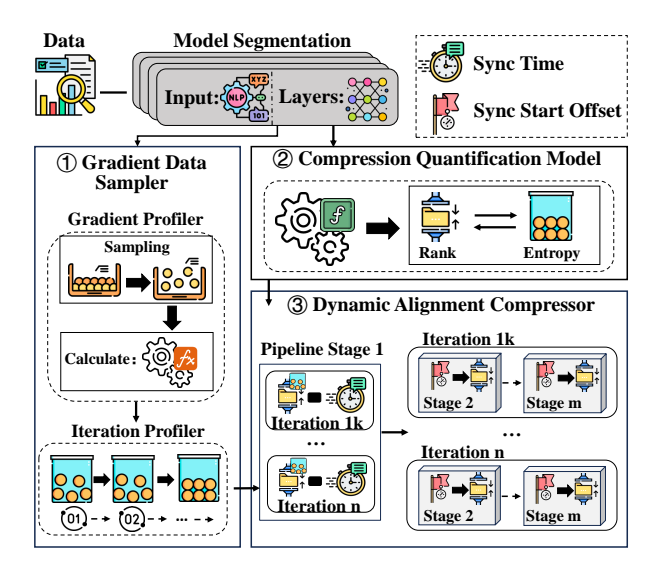


Fig. 5: Overview of EDGC

## IV. DESIGN OF EDGC

#### A. Overview

Considering the growing stability and centralization of LLM gradients, adjusting the compression rank based on their evolving patterns over time is more effective. To achieve this, we should focus on three key aspects: theory, implementation, and efficiency. First, accurately measuring variations in gradient information and identifying the appropriate compression rank for these changing gradients is vital. Second, as training LLMs often employs multiple parallel strategies, it is crucial to determine the right iterations, stages, and moments for applying compression. Third, efficiently implementing this dynamic compression method is a challenge.

To address these challenges, we propose EDGC, an entropy-driven dynamic gradient compression framework. As shown in Figure 5, EDGC consists of three main components: a gradient data sampler (GDS), a compression quantification model (CQM), and a dynamic alignment compressor (DAC). First, GDS handles large gradient data via a down-sampling technique that effectively captures gradient changes. Second, CQM serves as a theoretical model that establishes the relationship between compression rank and gradient entropy. Lastly, DAC dynamically adjusts the compression rank using a window mechanism and aligns compression ranks and initiation moments across different pipeline stages.

Additionally, we consider two key aspects of LLM training when designing EDGC. First, gradients exhibit significant variability during the initial phase, rendering compression ineffective. Thus, we implement a warm-up phase. Second, since training LLMs generally involves many iterations, adjusting the compression rate for each iteration is inefficient. We propose a window-based mechanism that monitors gradient change trends, allowing for the calculation of compression ranks at the window level. These features of EDGC are illustrated in Figure 6.

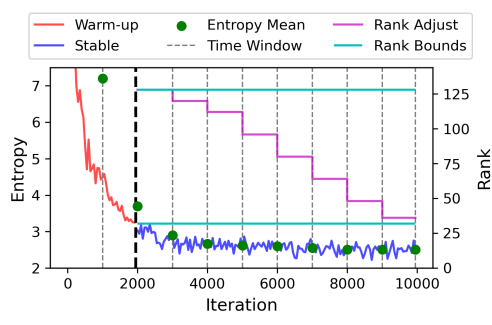


Fig. 6: Visualization of warm-up, entropy calculations, rank bounds, and window-based compression adjustments

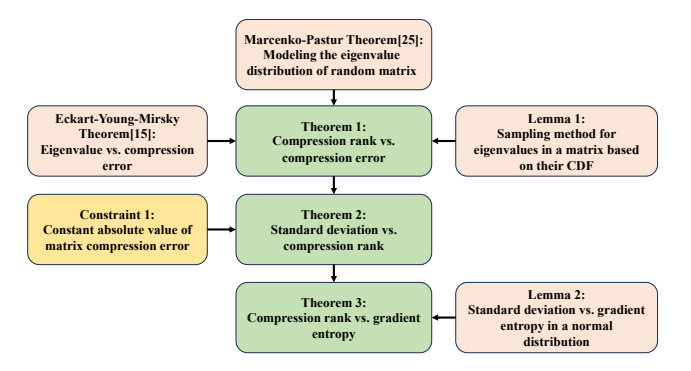


Fig. 7: The illustration of the CQM deduction process

# B. Gradient Data Sampler (GDS)

Considering the billions to trillions of parameters in LLMs, the main goal of GDS is to efficiently obtain a representative measure of gradients. It employs down-sampling at two levels: within a time window and during an iteration. First, GDS evaluates gradients at a specified iteration sampling rate (ISR), denoted as  $\alpha$ . Specifically, within each time window, gradient variation is calculated once every  $\frac{1}{\alpha}$  iterations. Second, GDS selects a data subset during an iteration based on a specific gradient sampling rate (GSR), represented as  $\beta$ . This approach significantly reduces the computational load, enabling rapid and accurate assessment of the gradient's condition while retaining essential information. Ablation studies presented in Section V-C1 demonstrate that GDS can decrease the time required for entropy calculation by approximately 94%.

#### C. Compression Quantification Model (CQM)

The precise quantification of the relationship between compression rank and gradient entropy remains underexplored, presenting a fundamental challenge that CQM aims to address. To clarify this, we outline the deduction process of CQM in Figure 7. The complete mathematical details and theoretical analysis are provided in Appendix A.

It is worth noting that, in our theoretical derivation (see Appendix A), we assume gradient components follow a normal distribution to enable tractable analysis. However, in practice, certain gradients may exhibit skewness or heavy tails during the early stages of training due to unstable optimization dynamics. Importantly, such deviations are typically transient and diminish as training progresses. The CQM framework

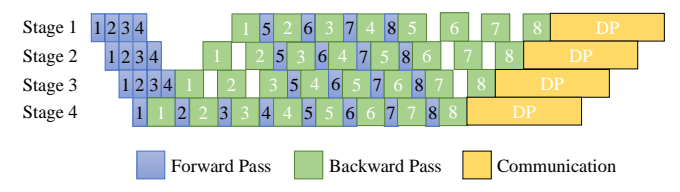


Fig. 8: Timing diagram of 3D parallelism

remains robust because its theoretical design inherently accommodates these temporary departures from normality. As shown in Observation 3, the actual compression error stays below the conservative theoretical upper bound—benefiting from gradient correlations—providing a reliable safety margin. Thus, the model maintains validity and effectiveness throughout the entire training process, even under evolving gradient distributions.

Based on Theorem 3, we propose an adjustment strategy that utilizes entropy and compression error perception to dynamically modify compression ranks during LLM training. However, frequent adjustments to the compression rank can lead to additional computational overhead, primarily due to the need for memory reallocation with each modification. To balance communication efficiency and computational costs, we introduce a window-based dynamic adjustment strategy.

## D. Dynamic Alignment Compressor (DAC)

As analyzed in Section II-A, two fundamental challenges in pipeline parallelism are identified: (1) temporal misalignment in parameter synchronization due to forward-backward dependencies, and (2) heterogeneous communication demands from uneven parameter distribution. Figure 8 demonstrates this through a 4-stage pipeline with eight micro-batches, where Stage 1's delayed backpropagation completion creates a synchronization bottleneck. DAC addresses these dual challenges through adaptive compression strategies with coordinated stage-level adjustments.

1) Computing Rank Bounds through the Link between Compression Rank and Communication Time: CQM defines the relationship between compression rank and DP communication performance by carefully selecting various ranks. To achieve temporal benefits in compression and decompression, the total communication time  $T_{com}$  for any specific rank must satisfy the following inequality:

$$T_{com} = T_{compress} + \frac{D_{compressed}}{B} + T_{decompress} \le \frac{D_{original}}{B}$$
 (2)

where  $T_{compress}$  denotes the time needed to compress data, while  $D_{compressed}$  indicates the amount of data after compression. B represents the network bandwidth. Furthermore,  $T_{decompress}$  is the time required to decompress data, and  $D_{original}$  signifies the volume of the original data before compression.

If the inequality is violated, compression fails to reduce communication time, defining the maximum allowable rank  $r_{max}$ . To ensure model accuracy and mitigate the negative effects of excessive compression, a lower rank limit  $r_{min}$ 

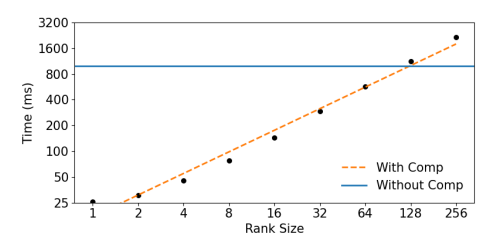


Fig. 9: Communication time with different rank values

should be established 1. Additionally, the link between compression rank and communication time is significantly affected by the hardware platform and network environment, rendering estimates based solely on a pre-trained model imprecise. To achieve more reliable communication time estimates, we gather real-time data, ensuring that results accurately reflect system behavior.

Based on real-time data from the pre-training of GPT2-2.5B, shown in Figure 9, we observe that different rank values r have an approximately linear relationship with the communication time  $T_{\text{com}}(r)$ . This experiment was conducted in a 32 Gbps bandwidth environment, with TP, PP, and DP set to 4, 4, and 2, respectively. Comprehensive hardware and network configurations for this setup are summarized in Cluster 1 of Table II.

Hence, to quantify this relationship, we model the communication time as a linear function of the compression rank:

$$T_{\rm com}(r) = \eta r \tag{3}$$

where  $\eta$  reflects the influence of compression rank on communication time. Empirical evaluation within the rank bounds shows a mean absolute percentage error (MAPE) of only 2.85%, suggesting that the linear model offers highly accurate predictions.

2) Adaptive Warm-up Phase Determination: As discussed in Section III, LLMs are sensitive to the precision of gradient updates during initial training. Early implementation of gradient compression can cause irreversible declines in model accuracy. To address this, EDGC initiates a warm-up phase where gradient compression is not applied. Additionally, it improves this process by adaptively defining the warm-up phase based on the compression error.

Specifically, before training, DAC estimates the initial maximum rank  $r_{max}$  and its error threshold  $\epsilon_{ini}$  using Eq. (3). During training, DAC computes the gradient entropy for each time window. A decrease in entropy signifies stabilization of the gradient distribution. Based on this change, DAC determines the new compression rank  $r_{new}$  for the current time window using Eq. (15). If  $r_{new} < r_{max}$ , the warmup phase ends, indicating that the gradient distribution has stabilized and the model is prepared for effective low-rank approximation. We also impose an empirical constraint to ensure model stability. A 10% warm-up phase is commonly used in practice to maintain convergence [49]. If the calculated warm-up phase is under 10% of the total iterations, we extend it to 10%. This approach prevents premature compression and better aligns with actual training conditions.

3) Window-based Rank Adjustment: Figure 10 presents our empirical analysis of gradient compression dynamics during GPT2-345M training. By monitoring layer-wise compression error, we observe three key phenomena. (1) Error decay property: the compression error under the same rank value gradually decreases. (2) Rank-error tradeoff: Under the same number of iterations, the smaller the rank, the larger the compression error. (3) Layer invariance: While absolute compression error magnitudes differ across layers, their relative error trends remain consistent.

Algorithm 1: Window-based Dynamic Rank Adjust-

```
Input: previous window rank r_{prev}, rank bounds
         [r_{\min}, r_{\max}], initial compression error \epsilon_{ini} at
```

**Output:** Updated rank  $r_{new}^{s_1}$  for pipeline stage 1 in w, and the predicted communication time  $T_{\text{com}}(r_{new}^{s_1})$ 

- 1 Configure adjustment limit s;
- 2 Calculate new rank  $r_{\text{new}}$  using Eq. (11) given  $\epsilon_{ini}$ ;

2 Calculate flew rain 
$$r_{\text{new}}$$
 using Eq. (11) given  $\epsilon_{ini}$ , 3 if  $|r_{new} - r_{prev}| > s$  then

4 | if  $r_{new} > r_{prev}$  then

5 |  $r_{new}^{s_1} = r_{\text{prev}} + s$ ;

6 | else

7 |  $r_{new}^{s_1} = r_{\text{prev}} - s$ ;

- 8 else
- $r_{new}^{s_1} = r_{\text{new}};$
- 10  $r_{new}^{s_1} = \max(r_{\min}, \min(r_{\max}, r_{new}^{s_1}));$
- 11 Predict communication time  $T_{\text{com}}(r_{new}^{s_1})$  using Eq. (3);
- 12 **return**  $r_{new}^{s_1}$  and  $T_{com}(r_{new}^{s_1})$ .

DAC exploits these properties through a three-phase adaptation. Firstly, the compression error of the predefined maximum rank  $r_{max}$  is calculated based on the initial gradients. Secondly, the average gradient entropy is computed in each time window w, and the compression direction is determined based on changes in the average entropy. If the average entropy decreases, indicating a more concentrated gradient distribution, the compression rank is reduced; otherwise, it is increased. Algorithm 1 formalizes this adaptive process through entropydriven rank adjustments constrained by empirically validated safety margins.

Constraint 2. (Rank adjustment limits.) To ensure smooth adjustments and mitigate performance impacts, a maximum adjustment limit s is established, enabling a seamless transition to the new compression rank. In our implementation, s is set

4) Stage-aligned Compression Rank Adjustment: Building on the estimated communication time of Stage 1, the compression ranks of subsequent pipeline stages can be adjusted to align their communication completion times with that of

<sup>&</sup>lt;sup>1</sup>Experiments suggest setting  $r_{min}$  within  $\left[\frac{r_{max}}{4}, \frac{r_{max}}{6}\right]$  effectively balances compression efficiency and model performance.

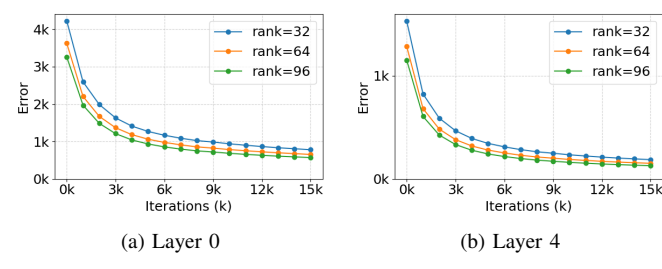


Fig. 10: Changes in compression error under different rank values during the iteration process

Stage 1. Let the communication time of Stage 1 be denoted as  $T_{\rm com}(r_{new}^{s_1})$ . The compression ranks for other stages i are then configured to maintain balance in the overall pipeline communication:

$$r_{new}^{s_i} = \frac{T_{\text{com}}}{\eta} = \frac{T_{\text{com}}(r_{new}^{s_1}) + (i-1) * \overline{T}_{\text{microBack}}}{\eta}$$
(4)

where i-1 represents the position offset between the i-th stage and Stage 1 in the pipeline.  $\overline{T}_{\text{microBack}}$  denotes the average time required for each stage to perform a micro-batch backpropagation.

To mitigate misalignment, it is essential to quantify and address time discrepancies between pipeline stages. The communication bottleneck occurs because Stage 1 initiates DP communication later than other stages due to sequential dependencies in backpropagation. By predicting the DP communication time for Stage 1 and the time differences at the start of communication for each stage, we can pinpoint the delay causing the bottleneck. Quantifying this misalignment enables DAC to adjust gradient compression ranks, balancing communication time across all stages. This strategy prevents an exclusive focus on Stage 1, which could inadvertently create new bottlenecks, while also maintaining model accuracy by appropriately relaxing compression ranks in other stages, thereby enhancing overall pipeline efficiency. Algorithm 2 presents this stage-aligned rank adjustment process.

# Algorithm 2: Stage-aligned Dynamic Rank Adjustment

**Input:** Communication time  $T_{\text{com}}(r_{new}^{s_1})$ , micro-batch backward time  $\overline{T}_{\text{microBack}}$ , rank bounds  $[r_{\min}, r_{\max}]$ 

**Output:** Compression rank  $r_{new}^{s_i}$  for each stage i

1 Initialize:  $r_{new}^{s_i} = r_{new}^{s_1}$  for each stage i;

2 foreach  $stage \ i \in \{2,3,\dots\}$  do

 $T_{\text{com}}^{s_i} = T_{\text{com}}(r_{new}^{s_1}) + (i-1) \times \overline{T}_{\text{microBack}};$ 

4 Compute rank  $r_{new}^{s_i}$  with  $T_{com}^{s_i}$  using Eq.(3);

6 return  $\{r_{new}^{s_i}\}$  for each stage i.

#### V. EVALUATION

# A. Experimental Setup

We assess the effectiveness of EDGC on two LLMs: GPT2-2.5B and GPT2-12.1B. These models are executed on an

TABLE II: Experimental environments

Cluster 1	Node	Number CPU Memory GPU	8 Xeon Platinum 8163, 32 cores 256 GB 4× Nvidia Tesla V100 (32 GB)	
	Interconnect	Intra-node Inter-node	NVLink (300 Gbps / GPU) Ethernet (32 Gbps)	
Cluster 2	Number CPU Memory GPU		16 Xeon Platinum 8558, 48 cores 512 GB 4× Nvidia H100 (80 GB)	
	Interconnect	Intra-node Inter-node	NVLink (900 Gbps / GPU) Infiniband NDR (400 Gbps)	
	Common	Micro-batch Total mini-batch Iterations	4 64 / 128 230,000	
Models	GPT2-2.5B	Layers Hidden dim Ways	52 1,920 TP4 / DP2 / PP4	
	GPT2-12.1B	Layers Hidden dim Ways	76 3,584 TP4 / DP4 / PP4	

8-node cluster and a 16-node cluster, respectively. Table II outlines the detailed configurations of nodes, networks, and LLMs.

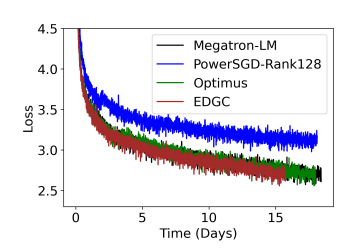
**Baselines**. We compare EDGC with three state-of-the-art methods: (1) Megatron-LM [61] is a baseline method without compression; (2) PowerSGD [66] uses low-rank decomposition for data compression; and (3) Optimus-CC [62] combines selection phase compression with low-rank decomposition and error feedback.

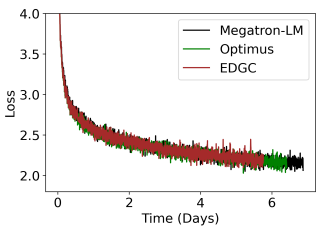
To systematically assess training performance and convergence speed, all methods undergo pre-training with over 230,000 iterations. Additionally, for both PowerSGD and Optimus-CC in GPT2-2.5B, we employed a default rank of 128, aligning with the Optimus-CC configuration. In GPT2-12.1B, the rank for PowerSGD and Optimus-CC is empirically set to 64 to optimize their performance.

**Model.** We chose GPT-2 as it is a well-established benchmark and representative medium-scale LLM, commonly used in prior work (e.g., Optimus-CC) for fair comparison. Midscale LLMs are also widely adopted in real-world applications, making our evaluation relevant.

**Datasets.** We used the OpenWebText [24] and OpenWebText2 [22] datasets for pre-training. The data was carefully preprocessed to maintain high quality and diversity. To evaluate the LLMs' generalization ability during training, we set aside 5% of the dataset as a validation set.

**Metrics.** We use communication time and training time to evaluate the training speed. In addition, we assess the performance of LLMs after pre-training using perplexity (PPL) and loss values. PPL is one of the most common indicators for evaluating language models. These metrics are consistent with those used in mainstream models [5], [47], [51], ensuring comparability of results.





- (a) Loss change on GPT2-2.5B
- (b) Loss change on GPT2-12.1B

Fig. 11: The change in loss over time

TABLE III: Training time and PPL after 230K iterations

Model	Metric	Megatron-LM	PowerSGD	Optimus-CC	EDGC
GPT2-2.5B	Time (day) PPL	18.44 17.95	18.14 22.37	18.01 17.97	15.74 17.95
GPT2-12.1B	Time (day) PPL	6.88 8.73	-	6.42 8.84	5.77 8.87

# B. Training Performance

1) LLM Convergence: Figure 11a and 11b illustrate the loss changes over time for GPT2-2.5B and GPT2-12.1B, respectively, under different methods. The results show that EDGC significantly outperforms the uncompressed scheme of Megatron-LM in terms of loss convergence speed, while achieving almost the same final loss value. These findings suggest that EDGC not only accelerates the convergence of LLMs, but also maintains strong generalization capability. Notably, in the GPT2-2.5B experiment, PowerSGD exhibited significantly worse performance, with both communication time and loss deviating considerably from those of Optimus-CC. Due to resource constraints, we did not include PowerSGD in the GPT2-12.1B experiment.

2) Training Speedup: Table III presents the training time and PPL of different methods after 230K iterations. The results show that EDGC significantly accelerates LLM training. For GPT2-2.5B, EDGC reduces training time by 14.64%, 13.23%, and 12.60% compared to Megatron-LM, PowerSGD, and Optimus-CC, respectively. Concretely, EDGC cuts communication time by 45.8% compared to Megatron-LM. For GPT2-12.1B, EDGC achieves a 16.13% and 10.12% reduction in training time relative to Megatron-LM and Optimus-CC, respectively. Similarly, communication time is reduced by 46.45% compared to Megatron-LM. Notably, GPT2-12.1B was trained on a 400GBps network, while GPT2-2.5B operated at just 32GBps. Even in high-bandwidth environments, where communication efficiency gains might be restricted, EDGC consistently shows acceleration. This suggests that EDGC can achieve substantial performance enhancements across various network conditions.

To further verify EDGC's scalability on larger-scale models, we conduct preliminary experiments on Llama-34B under a 400 Gbps high-speed interconnect using 32 GPUs (each with 64 GB of memory) in a bf16 precision setting with a distributed optimizer. After 10K iterations—corresponding to the early stage of training—EDGC achieves a 6% reduction in end-to-end training time and a 32.76% reduction in communication time compared to the baseline. Despite

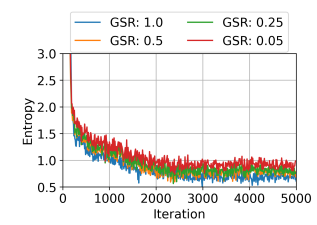
TABLE IV: Accuracies on zero-shot tasks

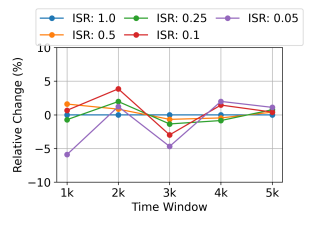
Tasks		GPT2-2.5B				GPT2-12.1B		
	Megatron	Pow-SGD	Opti-CC	EDGC	Mega	Opti-CC	EDGC	
ARC_easy	41.75%	41.67%	41.73%	40.95%	60.65%	59.84%	58.25%	
ARC_challenge	21.84%	21.08%	21.84%	21.76%	28.84%	26.59%	27.47%	
HellaSwag	35.55%	30.24%	35.41%	35.64%	42.34%	42.01%	40.65%	
OpenBookQA	20.00%	17.40%	20.80%	21.20%	24.60%	25.01%	23.40%	
PIQA	65.23%	63.28%	65.23%	65.23%	72.25%	70.50%	70.35%	
WinoGrande	51.62%	50.99%	51.99%	52.25%	58.88%	57.89%	57.62%	

adopting conservative gradient compression during the early training phase to maintain convergence stability, EDGC still delivers notable communication efficiency gains. As training progresses and convergence becomes more stable, EDGC incrementally applies more aggressive compression, which is expected to yield further acceleration. While these results represent an early-stage snapshot, they demonstrate EDGC's scalability and indicate substantial potential for enhanced efficiency as training converges.

For GPT2-2.5B, both EDGC and Megatron-LM achieve a PPL of 17.95, demonstrating that EDGC shortens training time while maintaining model quality. This supports our earlier Observation 3, which noted correlations among gradient matrices. These correlations ensure that the actual compression error in EDGC is lower than the theoretical error, effectively preserving model performance. PowerSGD yields a PPL of 22.37, indicating that static low-rank decomposition may hinder model performance. Optimus-CC exhibits a PPL of 17.97, comparable to EDGC and Megatron-LM. For GPT2-12.1B. both EDGC and Optimus-CC show a minor rise, about 0.1, in PPL relative to Megatron-LM. This is acceptable due to the notable enhancement in communication efficiency. Even when trained to reach the same perplexity as the baseline, EDGC consistently delivers substantial end-to-end efficiency gains. Specifically, to match the baseline PPL, EDGC requires only approximately 0.4% more iterations for GPT2-2.5B and 2.1% for GPT2-12.1B, while still achieving 14.30% and 14.37% overall speedup, respectively. Consequently, EDGC maintains model quality while substantially accelerating large-scale pretraining across diverse model sizes and network conditions.

3) Accuracies on Zero-shot Tasks: We evaluated LLMs' performance on zero-shot tasks, highlighting their generalizability. Table IV shows accuracy for various tasks including ARC\_easy [8], ARC\_challenge [8], HellaSwag [74], Open-BookQA [41], PIQA [3], and WinoGrande [55]. The results for GPT2-2.5B fall within an acceptable range of training randomness, indicating that EDGC consistently matches the accuracies of Megatron-LM on these tasks. For GPT2-12.1B, EDGC achieves performance that is generally comparable to Megatron-LM on zero-shot tasks, though slight differences are observed on certain benchmarks. These discrepancies may arise from the limited training iterations. To enable a fair comparison, we adhered to the same 230K iteration schedule used in Optimus-CC, instead of the full 500K iterations from Megatron-LM's original setup. This shorter training duration may have resulted in underfitting on certain benchmarks, especially for large-scale models that need longer training to fully converge. As the model converges with additional iterations, the gradients hold less information (i.e., lower entropy).





- ferent gradient sampling rates
- (a) Gradient entropy changes at dif- (b) Relative change rate of entropy in different time windows

Fig. 12: Entropy and its relative change rate over iterations

TABLE V: Time cost under different GSRs ( $\beta$ )

	β <b>=1.0</b>	β <b>=0.5</b>	β=0.25	β=0.05
Calculation Time (ms)	78.14	58.7	46.85	39.93

This enables EDGC to achieve higher compression rates with minimal accuracy loss, resulting in significant communication savings, even during extended training.

## C. Ablation Studies

EDGC consists of three modules: GDS, CQM, and DAC. We evaluate their effects using thorough ablation studies.

1) Analysis of GDS: To evaluate the impact of sampling rates on entropy estimation and computational efficiency, we experimented with different gradient sampling rates (GSR)  $\beta$ and iteration sampling rates (ISR)  $\alpha$  using BERT-345M. We first varied  $\beta$  (0.05, 0.25, 0.5, 1.0) and computed gradient entropy over 5,000 iterations using Eq. (1). As shown in Figure 12a, even small values of  $\beta$  effectively captured the entropy dynamics, with  $\beta = 0.25$  offering a good trade-off between accuracy and overhead. With  $\beta$  fixed at 0.25, we then explored different  $\alpha$  values (0.05, 0.1, 0.25, 0.5). Figure 12b reports the relative change rate (RCR) of average entropy per 1,000iteration window, using  $\alpha = 1$  as the baseline. Results show that overly low  $\alpha$  (e.g., 0.05) leads to RCR above 5%, whereas  $\alpha = 0.1$  yields stable estimates with minimal deviation.

To assess the efficiency benefits, we further measured the entropy computation time under different  $\beta$  values per iteration, as shown in Table V. When  $\beta = 0.25$ , the time cost drops by 40% compared to the full data scenario. Combined with  $\alpha = 0.1$ , the total entropy estimation time within each time window is reduced by approximately 94%, significantly improving overall training efficiency.

2) Analysis of COM: Using GPT2-345M, we compare CQM with three fixed-rank low-rank methods (64, 32, and 16) and a no-compression baseline. All models were trained under the same conditions, assessing PPL on the validation set every 1,000 iterations to gauge model accuracy and convergence speed. Notably, Rank=64 is the threshold  $r_{\text{max}}$ , where communication starts to benefit from compression, while Rank=16 is the minimum allowable value  $r_{\min}$ . CQM dynamically selects rank within this range to reduce communication time while maintaining model accuracy.

As shown in Figure 13, smaller ranks cause more information loss due to aggressive compression. In particular, the Rank=16 strategy results in significantly higher PPL values

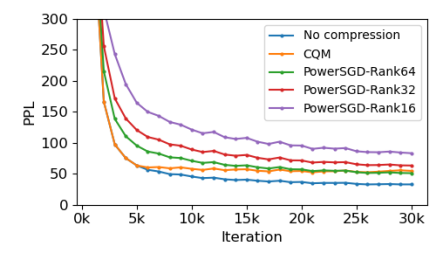


Fig. 13: PPL trend under different compression strategies

TABLE VI: Communication time over 30,000 training steps

Method	No Compression	Rank=64	Rank=32	Rank=16	CQM (Ours)
Time (h)	3.0417	3.0167	1.4833	0.7417	1.8750

throughout training, indicating that excessive compression severely limits the model's expressive capacity. Rank=64 maintains better accuracy but does not bring significant communication benefits. In contrast, the COM curve demonstrates a clear advantage. In the early training stages, thanks to the adaptive warm-up determination mechanism in our EDGC framework, the model benefits from full-precision updates to ensure stable convergence and sufficient quality accumulation. Afterwards, CQM adjusts the rank based on gradient dynamics, gradually approaching the performance of Rank=64 in terms of PPL, while maintaining significantly lower communication costs, as shown in Table VI. This confirms the effectiveness of our dynamic rank adaptation strategy.

3) Analysis of DAC: To evaluate the impact of window size on adaptive rank adjustment, we conduct a systematic analysis using BERT-345M and GPT-2-345M models. Specifically, we measure the fidelity of entropy dynamics across different update intervals. Rank adaptation occurs periodically at the end of each w-iteration window, with updates guided by the evolution of gradient entropy within the window. We use a fine-grained schedule with w=1, where rank is updated every iteration, as the baseline for temporal fidelity. We quantify the similarity between the entropy change trajectories for different window sizes (w) and the w = 1 baseline using correlation coefficient (CC) and mean squared error (MSE). As shown in Table VII, a window size of w = 1000 strikes an optimal balance: it preserves strong temporal alignment (CC = 0.9433 for BERT and 0.9807 for GPT-2) with minimal deviation (MSE < 0.3), while significantly reducing the frequency of rank updates. In contrast, a larger window size of w = 2500 introduces noticeable distortion in entropy dynamics, particularly for BERT. These findings demonstrate that w = 1000 effectively balances the trade-off between estimation fidelity and computational efficiency. It captures the key entropy variations with sufficient resolution, without incurring excessive adaptation overhead. Consequently, we adopt w = 1000 as the default window size in our framework.

To validate the effectiveness of the stage-aware alignment mechanism, we conduct experiments on GPT-2-345M, comparing the full DAC method with an ablated variant where stage-aware alignment is disabled. In the ablated baseline, all pipeline stages share a globally synchronized rank that

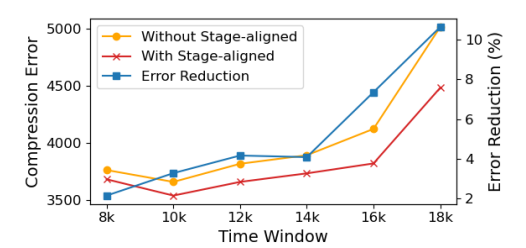


Fig. 14: Effect of Stage-aligned on compression error

TABLE VII: Performance metrics (CC, MSE) for varying time window sizes(w)

Metric	Model	w=1	w=100	w=500	w=1000	w=2500
CC	BERT GPT-2	1.0000 1.0000	0.9891 0.9979	0.9838 0.9920	0.9433 0.9807	0.8004 0.9634
MSE		0.0000 0.0000	0.0059 0.0066	0.0534 0.0288	0.2742 0.1561	1.2181 0.8750

is periodically updated, limiting the adaptability to stagespecific gradient characteristics. As shown in Figure 14, the full DAC method consistently achieves lower compression error throughout training. Notably, the absolute compression error in both the full DAC and ablated variants increases over time, which aligns with the expected behavior. Specifically, DAC reduces the rank progressively to enhance compression efficiency, particularly in later stages that can tolerate lower gradient fidelity. However, by leveraging stage-aligned rank adaptation, DAC more accurately captures the heterogeneous evolution of gradient entropy across layers, leading to superior reconstruction accuracy. The relative error reduction—defined as the percentage improvement of DAC over the ablated baseline—steadily increases during training and surpasses 10% by 18k iterations. This trend suggests that stage-aware compression becomes increasingly advantageous as the model evolves, allowing finer-grained control over per-stage precision.

# VI. DISCUSSION

EDGC demonstrates generalizability in four key aspects. (1) While compression inevitably causes some information loss, EDGC minimizes this by balancing training cost and model performance. For instance, to reach the same PPL as the uncompressed baseline at 230K iterations, EDGC needs only 0.4% and 2.1% more iterations for GPT-2 2.5B and 12.1B, respectively. Despite this, overall training time is still reduced by 14.30% and 14.37%, due to significant communication savings. (2) EDGC can be integrated into various parallel training paradigms for LLMs. While 3D parallelism is common, our approach can also apply to mixture-of-experts (MOE) models, typically regarded as 4D parallelism, where communication patterns is even more intricate. (3) The advantages of EDGC are particularly evident in bandwidth-limited environments. In the network setup for training GPT2-12.1B with a bandwidth of 400Gbps, communication time accounts for around 34% of the total training duration. However, when the bandwidth decreases to 32Gbps, the proportion of communication time increases sharply to about 87%. In these bandwidth-constrained situations, communication overhead becomes a major bottleneck for training performance. Implementing dynamic gradient compression can significantly reduce data transmission, leading to notable enhancements in training efficiency. (4) As LLMs expand, the synchronization of parameters rises, resulting in increased communication overhead. EDGC's adaptive compression strategy effectively mitigates these bottlenecks in large systems. While EDGC did not examine larger models or more extensive configurations due to the associated high costs, the results highlight the promising potential of EDGC in improving the training efficiency of LLMs.

#### VII. RELATED WORK

As shown in Table VIII, many studies focus on optimizing communication in LLM training.

Firstly, overlapping computation with communication can minimize waiting times [59], [60], [76]. For instance, WFBP [76] leverages the neural network structure to compute updates for lower layers while transmitting top-level parameter updates, effectively masking much of the communication delay. IPart [69] integrates the communication and computational overhead characteristics of layers to refine the merging strategy. However, these algorithms become less effective when there is a significant disparity between computation and communication costs and heavily depend on precise layer merging strategies.

Secondly, some studies have used semi-synchronous methods (e.g., Stale Synchronous Parallelism (SSP [29]), Spec-Sync [75], and Eager-SGD [37] to enhance communication efficiency. For example, SSP allows certain nodes to tolerate delays, enabling them to keep computing even when updates are unsynchronized, thus reducing time lost due to waiting for synchronization. While these methods show significant improvements in communication efficiency, the challenge remains in balancing efficiency with model accuracy and convergence, as asynchronous updates may introduce gradient discrepancies. Ensuring both performance and convergence under these conditions is a primary challenge for these approaches.

Thirdly, several studies, including 1-bit Adam [64], SliceGPT [1], Top-k Allreduce [38], Optimus-CC [62], and DeepSeek-V3 [39], have introduced techniques to minimize communication data, such as low-precision calculations [2], [10], [56] and gradient sparsification [16], [58], [63], [70]. These methods improve communication efficiency by reducing the data exchanged. However, they often lead to decreased model accuracy. Notably, low-precision techniques like 1-bit Adam, while significantly reducing communication time, can adversely impact the final performance of LLMs.

EDGC combines gradient compression with an error feed-back mechanism, dynamically adjusting the compression rate based on gradient evolution trends. This information theory-driven method provides notable communication benefits while preserving model accuracy and ensuring convergence speed.

## VIII. CONCLUSIONS

In this work, we propose EDGC, an entropy-driven dynamic gradient compression strategy aimed at enhancing communi-

TABLE VIII: Communication optimization methods for LLM

Method	Optimization Type	Theoretical/Emprical	Adaptability
WFBP [76] MG-WFBP [60]	Comp-Comm Overlap	Emprical Theoretical	No No
IPart [69]	сопр-соппп оченар	Theoretical	No
SSP [29]		Theoretical	No
SpecSync [75]	Semi-Synchronous	Emprical	Yes
Eager-SGD [37]	Seim Synemonous	Theoretical	No
1-bit Adam [64]		Theoretical	No
Top-k Allreduce [38]		Theoretical	No
SliceGPT [1]	Gradient Compression	Emprical	No
Optimus-CC [62]	-	Emprical	No
EDGC(ours)		Theoretical	Yes

cation efficiency in large, distributed models. Current communication compression methods often fail to adapt to changing training conditions, resulting in inefficient communication and possible declines in model quality. To tackle these challenges, we introduced several innovative techniques, including adaptive compression threshold estimation, a dynamic warm-up mechanism, periodic compression ratio adjustments, and a layered compression strategy. These techniques effectively reduce communication overhead during training while preserving model accuracy.

#### APPENDIX

#### A. Detailed Derivations for CQM

We introduce two established theorems to support the proof of our derived theorems.

Lemma 1. (CDF of the Marchenko-Pastur Distribution) Marcenko-Pastur Theorem [25] describes the asymptotic behavior of the eigenvalues of large random covariance matrices. Given a matrix  $A \in \mathbb{R}^{m \times n}$  and the standard deviation of each entry in A is equal to 1, the cumulative distribution function (CDF) of  $AA^T$ 's eigenvalue  $\lambda$  satisfies:

$$F(\lambda; m, n) = \frac{1}{2\pi m} F(\lambda; a, b)$$
 (5) with  $a = (\sqrt{n} - \sqrt{m})^2$ ,  $b = (\sqrt{n} + \sqrt{m})^2$ , and 
$$F(\lambda; a, b) = -2\sqrt{ab} \arctan\left(\sqrt{\frac{b(\lambda - a)}{a(b - \lambda)}}\right) + (a + b) \arcsin\left(\sqrt{\frac{\lambda - a}{b - a}}\right) + \sqrt{(\lambda - a)(b - \lambda)}.$$

The proof of this lemma spans approximately one page. Due to the length constraint and the overall structure, it will be presented later.

Theorem 1. (Relationship between Compression Rank and Compression Error.) Suppose that there is a random gradient matrix<sup>2</sup>  $A \in \mathbb{R}^{m \times n}$  with entries that are i.i.d., having mean 0 and variance 1. When the compression rank is set to r, the squared compression error  $||A - A_r||_F^2$  can be estimated as follows:

a) Compute a and b from Lemma 1, and uniformly sample values  $\{\lambda_0\}$  within the range from a to b;

- b) Determine the corresponding cumulative probabilities  $\{p_0\}$  based on the CDF  $F(\lambda_0)$  in Lemma 1 to create pairs  $\{(\lambda_0, p_0)\}$ ;
- c) Randomly sample m values  $\{p\}$  from a uniform distribution (0,1) to find the corresponding  $\{\lambda\}$  from the pairs  $\{(\lambda_0, p_0)\}$ , where  $\{\lambda\}$  represent the sampled eigenvalues;
- d) Calculate the sum of the smallest m-r values in  $\{\lambda\}$  as the estimation of the squared compression error.

*Proof.* Noting that the squares of the singular values of matrix A equal the eigenvalues of  $AA^T$ , if  $A_r$  represents the best rank-r approximation of A, according to the Eckart-Young-Mirsky Theorem [15], the matrix squared compression error measured by the Frobenius norm satisfies:

$$||A - A_r||_F^2 = \sum_{i=r+1}^m \lambda_i,$$
 (6)

which corresponds to the sum of the last m-r eigenvalues of  $AA^T$ .

Furthermore, according to Lemma 1 and the Marcenko-Pastur Theorem [25], the distribution of the eigenvalues of  $AA^T$  is defined in Eq. (5). Since directly calculating the analytical solutions for  $||A-A_r||_F^2$  is challenging, Monte Carlo sampling methods can be used to derive statistical results. The sampling results  $\{\lambda\}$  after steps a), b) and c) serve as an unbiased estimation of the m eigenvalues of  $AA^T$ .

Therefore, the sum of the smallest m-r values in  $\{\lambda\}$  provides an unbiased estimation of compression error  $||A-A_r||_F^2$ .

This theorem provides a practical method for estimating the compression error  $\epsilon = ||A - A_r||_F$  based on the compression rank r and the dimensions (m,n) of a random gradient matrix with standard normal entries. This process can be formalized as:

$$\epsilon = q(r; m, n). \tag{7}$$

As noted in Observation 3, inherent correlations exist among gradient matrices during training. These correlations stem from the backpropagation mechanism and parameter coupling, indicating that gradient information is partially redundant. Therefore, when using compression techniques, the actual information loss-i.e., the practical compression error-is often lower than the theoretical compression error predicted under the i.i.d. or uncorrelated assumption. This helps maintain the performance of LLMs during compression.

Constraint 1. (Constant absolute value of gradient matrix compression error.) To facilitate the adjustment of compression ranks, we impose a fixed compression error  $\epsilon_{ini}$  constraint during LLM training. This error is established when gradient compression is activated, as detailed in Section IV-D2.

Theorem 2. (Relationship between Compression Rank and Standard Deviation.) Let  $\sigma_0$  denote the standard deviation of a random gradient matrix  $A \in \mathbb{R}^{m \times n}$ . The compression error  $\epsilon = ||A - A_r||_F$  adheres to Constraint 1 throughout the training process. If the standard deviation shifts from  $\sigma_0$  to  $\sigma_1$ 

<sup>&</sup>lt;sup>2</sup>LLM parameters are typically initialized to random values.

during LLM training, the compression rank can be adjusted from  $r_0$  to  $r_1$  by:

$$r_1 = g^{-1} \left( \frac{\sigma_0}{\sigma_1} g(r_0) \right).$$

*Proof.* For a random gradient matrix A with a standard deviation of  $\sigma_0$ , setting the compression rank to  $r_0$  results in a compression error  $\epsilon$ . By maintaining  $\epsilon$ , as the matrix transitions from A to A' during LLM training, the standard deviation decreases to  $\sigma_1$  ( $\sigma_1 < \sigma_0$ ). The norm of the matrix A' is given by:

$$\frac{||A'||_F}{||A||_F} = \frac{\sigma_1}{\sigma_0}.$$
 (8)

When the compression rank is fixed to r, the relationship between compression error and standard deviation is established as:  $\epsilon_0 \sigma_1 = \epsilon_1 \sigma_0$ , which indicates that:

$$\epsilon \propto g(r; m, n)\sigma.$$
 (9)

Therefore, if the absolute compression error of gradient matrices remains constant, i.e.,  $||A - A_r||_F = ||A' - A'_r||_F$ , the error rate relationship for the matrix decomposition is given by:

$$g(r_0)\sigma_0 = g(r_1)\sigma_1. \tag{10}$$

Thus, the rank  $r_1$  can be determined as follows:

$$r_1 = g^{-1} \left( \frac{\sigma_0}{\sigma_1} g(r_0) \right). \tag{11}$$

Lemma 2. Relationship between Gradient Entropy and Standard Deviation. For a random variable X which follows a normal distribution with mean  $\mu$  and standard deviation  $\sigma$ , its information entropy is given by:

$$H(X) = \log \sigma + \frac{1}{2} \log 2\pi e. \tag{12}$$

*Proof.* Suppose a random variable X follows a normal distribution with mean 0 and variance 1. Based on Eq. (1),

$$H(X) = -\int f(x) \log f(x) dx$$

$$= \int \frac{1}{\sqrt{2\pi}\sigma} e^{-\frac{(x-\mu)^2}{2\sigma^2}} \left( \log(\sqrt{2\pi}\sigma) + \frac{(x-\mu)^2}{2\sigma^2} \right) dx$$

$$= \log(\sqrt{2\pi}\sigma) \int \frac{1}{\sqrt{2\pi}\sigma} e^{-\frac{(x-\mu)^2}{2\sigma^2}} dx$$

$$+ \int \frac{(x-\mu)^2}{2\sigma^2} \frac{1}{\sqrt{2\pi}\sigma} e^{-\frac{(x-\mu)^2}{2\sigma^2}} dx.$$

The first term corresponds to the probability density function of the normal distribution, which integrates to 1. For the second term, let  $x=y\sigma+\mu$ , then  $dx=\sigma dy$ , and the integral transforms into:

$$\begin{split} H(X) &= \log(\sqrt{2\pi}\sigma) + \frac{1}{2} \int y^2 \frac{1}{\sqrt{2\pi}} e^{-\frac{y^2}{2}} dy \\ &= \log(\sqrt{2\pi}\sigma) + \frac{1}{2} \\ &= \log \sigma + \frac{1}{2} \log 2\pi e. \end{split}$$

As noted in Observation 2, gradient distributions tend to centralize as training progresses and can be well-approximated by a normal distribution. Under this assumption, Lemma 2 shows that entropy is directly linked to the standard deviation, implying that reduced gradient variance corresponds to lower entropy. This provides a theoretical basis for tracking training dynamics via entropy.

Theorem 3. (Relationship between Compression Rank and Gradient Entropy) During the training process, suppose the gradient entropy of matrix A changes from  $H_0$  to  $H_1$ , the rank should be adjusted from  $r_0$  to  $r_1$  with a fixed error, which satisfies

$$r_1 = g^{-1} \left( e^{H_0 - H_1} g(r_0) \right).$$

*Proof.* Based on Lemma 2, the entropy of a random variable that follows a normal distribution is a logarithmic function of its standard deviation  $\sigma$ . Consequently, if the standard deviation of the gradient matrix shifts from  $\sigma_0$  to  $\sigma_1$ , the variation in entropy is:

$$H_1 - H_0 = \log \frac{\sigma_1}{\sigma_0}. (13)$$

Rearranging the equation yields:

$$\frac{\sigma_0}{\sigma_1} = e^{H_0 - H_1}. (14)$$

Since the compression rank depends on the standard deviation, applying Theorem 2 yields:

$$r_1 = g^{-1} \left( e^{H_0 - H_1} g(r_0) \right).$$
 (15)

#### REFERENCES

- [1] S. Ashkboos, M. L. Croci, M. G. D. Nascimento, T. Hoefler, and J. Hensman, "Slicegpt: Compress large language models by deleting rows and columns," in *The Twelfth International Conference on Learning Representations (ICLR)*, 2024. [Online]. Available: https://openreview.net/forum?id=vXxardq6db
- [2] J. Bernstein, Y. Wang, K. Azizzadenesheli, and A. Anandkumar, "SIGNSGD: compressed optimisation for non-convex problems," in Proceedings of the 35th International Conference on Machine Learning (ICML), ser. Proceedings of Machine Learning Research, vol. 80, 2018, pp. 559–568. [Online]. Available: http://proceedings.mlr.press/ v80/bernstein18a.html
- [3] Y. Bisk, R. Zellers, J. Gao, Y. Choi et al., "Piqa: Reasoning about physical commonsense in natural language," in Proceedings of the AAAI conference on artificial intelligence, vol. 34, no. 05, 2020, pp. 7432– 7439.
- [4] S. Black, S. Biderman, E. Hallahan, Q. G. Anthony, L. Gao, L. Golding, H. He, C. Leahy, K. McDonell, J. Phang, M. M. Pieler, U. S. Prashanth, S. Purohit, L. Reynolds, J. Tow, B. Wang, and S. Weinbach, "Gpt-neox-20b: An open-source autoregressive language model," ArXiv, vol. abs/2204.06745, 2022. [Online]. Available: https://api.semanticscholar.org/CorpusID:248177957

- [5] T. B. Brown, B. Mann, N. Ryder, M. Subbiah, J. Kaplan, P. Dhariwal, A. Neelakantan, P. Shyam, G. Sastry, A. Askell, S. Agarwal, A. Herbert-Voss, G. Krueger, T. Henighan, R. Child, A. Ramesh, D. M. Ziegler, J. Wu, C. Winter, C. Hesse, M. Chen, E. Sigler, M. Litwin, S. Gray, B. Chess, J. Clark, C. Berner, S. McCandlish, A. Radford, I. Sutskever, and D. Amodei, "Language models are few-shot learners," in Proceedings of the 34th International Conference on Neural Information Processing Systems, ser. NIPS '20, 2020, pp. 1877–1901.
- [6] C. Chen, W. Wang, and B. Li, "Round-robin synchronization: Mitigating communication bottlenecks in parameter servers," in *IEEE INFOCOM* 2019 - *IEEE Conference on Computer Communications*, 2019, pp. 532– 540.
- [7] C.-Y. Chen, J. Ni, S. Lu, X. Cui, P.-Y. Chen, X. Sun, N. Wang, S. Venkataramani, V. Srinivasan, W. Zhang, and K. Gopalakrishnan, "Scalecom: scalable sparsified gradient compression for communication-efficient distributed training," in *Proceedings of the 34th International Conference on Neural Information Processing Systems*, ser. NIPS '20, 2020, pp. 13551–13563.
- [8] P. Clark, I. Cowhey, O. Etzioni, T. Khot, A. Sabharwal, C. Schoenick, and O. Tafjord, "Think you have solved question answering? try arc, the ai2 reasoning challenge," ArXiv, vol. abs/1803.05457, 2018. [Online]. Available: https://api.semanticscholar.org/CorpusID:3922816
- [9] J. Dean, G. S. Corrado, R. Monga, K. Chen, M. Devin, Q. V. Le, M. Z. Mao, M. Ranzato, A. Senior, P. Tucker, K. Yang, and A. Y. Ng, "Large scale distributed deep networks," in *Proceedings of the 26th International Conference on Neural Information Processing Systems - Volume 1*, ser. NIPS'12, 2012, p. 1223–1231.
- [10] T. Dettmers, "8-bit approximations for parallelism in deep learning," CoRR, vol. abs/1511.04561, 2015. [Online]. Available: https://api.semanticscholar.org/CorpusID:15201887
- [11] J. Devlin, M.-W. Chang, K. Lee, and K. Toutanova, "BERT: Pre-training of deep bidirectional transformers for language understanding," in Proceedings of the 2019 Conference of the North American Chapter of the Association for Computational Linguistics: Human Language Technologies, Volume 1 (Long and Short Papers), 2019, pp. 4171–4186. [Online]. Available: https://aclanthology.org/N19-1423/
- [12] N. Du, Y. Huang, A. M. Dai, S. Tong, D. Lepikhin, Y. Xu, M. Krikun, Y. Zhou, A. W. Yu, O. Firat, B. Zoph, L. Fedus, M. Bosma, Z. Zhou, T. Wang, Y. E. Wang, K. Webster, M. Pellat, K. Robinson, K. S. Meier-Hellstern, T. Duke, L. Dixon, K. Zhang, Q. V. Le, Y. Wu, Z. Chen, and C. Cui, "Glam: Efficient scaling of language models with mixture-of-experts," ArXiv, vol. abs/2112.06905, 2021. [Online]. Available: https://api.semanticscholar.org/CorpusID:245124124
- [13] J. Duan, S. Zhang, Z. Wang, L. Jiang, W. Qu, Q. Hu, G. Wang, Q. Weng, H. Yan, X. Zhang, X. Qiu, D. Lin, Y. Wen, X. Jin, T. Zhang, and P. Sun, "Efficient training of large language models on distributed infrastructures: A survey," *CoRR*, vol. abs/2407.20018, 2024. [Online]. Available: https://doi.org/10.48550/arXiv.2407.20018
- [14] A. Dubey, A. Jauhri, A. Pandey, A. Kadian, A. Al-Dahle, A. Letman, A. Mathur, A. Schelten, A. Yang, A. Fan et al., "The llama 3 herd of models," CoRR, vol. abs/2407.21783, 2024. [Online]. Available: https://doi.org/10.48550/arXiv.2407.21783
- [15] C. Eckart and G. Young, "The approximation of one matrix by another of lower rank," *Psychometrika*, vol. 1, no. 3, p. 211–218, 1936.
- [16] J. Fang, H. Fu, G. Yang, and C.-J. Hsieh, "Redsync: Reducing synchronization bandwidth for distributed deep learning training system," *Journal of Parallel and Distributed Computing*, vol. 133, pp. 30–39, 2019. [Online]. Available: https://www.sciencedirect.com/ science/article/pii/S0743731518308657
- [17] W. Fedus, B. Zoph, and N. Shazeer, "Switch transformers: Scaling to trillion parameter models with simple and efficient sparsity," *J. Mach. Learn. Res.*, vol. 23, pp. 120:1–120:39, 2022. [Online]. Available: https://jmlr.org/papers/v23/21-0998.html
- [18] Z. Feng, D. Guo, D. Tang, N. Duan, X. Feng, M. Gong, L. Shou, B. Qin, T. Liu, D. Jiang, and M. Zhou, "CodeBERT: A pre-trained model for programming and natural languages," in *Findings of the Association for Computational Linguistics: EMNLP 2020*, 2020, pp. 1536–1547. [Online]. Available: https://aclanthology.org/2020.findings-emnlp.139/
- [19] W. Foundation, "Wikimedia downloads," [Accessed 09-04-2025]. [Online]. Available: https://dumps.wikimedia.org
- [20] S. Fox, S. Rasoulinezhad, J. Faraone, D. Boland, and P. H. W. Leong, "A block minifloat representation for training deep neural networks," in 9th International Conference on Learning Representations (ICLR), 2021. [Online]. Available: https://openreview.net/forum?id=6zaTwpNSsQ2

- [21] D. D. Freitas, M.-T. Luong, D. R. So, J. Hall, N. Fiedel, R. Thoppilan, Z. Yang, A. Kulshreshtha, G. Nemade, Y. Lu, and Q. V. Le, "Towards a human-like open-domain chatbot," *ArXiv*, vol. abs/2001.09977, 2020. [Online]. Available: https://api.semanticscholar.org/CorpusID: 210920238
- [22] L. Gao, S. Biderman, S. Black, L. Golding, T. Hoppe, C. Foster, J. Phang, H. He, A. Thite, N. Nabeshima, S. Presser, and C. Leahy, "The Pile: An 800gb dataset of diverse text for language modeling," arXiv preprint arXiv:2101.00027, 2020.
- [23] A. Gibiansky, "Bringing HPC Techniques to Deep Learning," https://andrew.gibiansky.com/blog/machine-learning/baidu-allreduce, 2017, [Accessed 09-04-2025].
- [24] A. Gokaslan, V. Cohen, E. Pavlick, and S. Tellex, "Openwebtext corpus," http://Skylion007.github.io/OpenWebTextCorpus, 2019, [Accessed 09-04-2025]
- [25] F. Götze and A. N. Tikhomirov, "Rate of convergence in probability to the marchenko-pastur law," *Bernoulli*, vol. 10, pp. 503–548, 2004. [Online]. Available: https://api.semanticscholar.org/CorpusID: 119916628
- [26] P. Goyal, P. Dollár, R. B. Girshick, P. Noordhuis, L. Wesolowski, A. Kyrola, A. Tulloch, Y. Jia, and K. He, "Accurate, large minibatch sgd: Training imagenet in 1 hour," ArXiv, vol. abs/1706.02677, 2017. [Online]. Available: https://api.semanticscholar.org/CorpusID:13905106
- [27] S. Gunasekar, J. Lee, D. Soudry, and N. Srebro, "Characterizing implicit bias in terms of optimization geometry," in *Proceedings of the* 35th International Conference on Machine Learning, ser. Proceedings of Machine Learning Research, vol. 80, 2018, pp. 1832–1841. [Online]. Available: https://proceedings.mlr.press/v80/gunasekar18a.html
- [28] J. He, J. Zhai, T. Antunes, H. Wang, F. Luo, S. Shi, and Q. Li, "Fastermoe: modeling and optimizing training of largescale dynamic pre-trained models," in *Proceedings of the 27th* ACM SIGPLAN Symposium on Principles and Practice of Parallel Programming, ser. PPoPP '22, 2022, p. 120–134. [Online]. Available: https://doi.org/10.1145/3503221.3508418
- [29] Q. Ho, J. Cipar, H. Cui, J. K. Kim, S. Lee, P. B. Gibbons, G. A. Gibson, G. R. Ganger, and E. P. Xing, "More effective distributed ml via a stale synchronous parallel parameter server," in *Proceedings of the 27th International Conference on Neural Information Processing Systems Volume 1*, ser. NIPS'13, 2013, p. 1223–1231.
- [30] Y. Huang, Y. Cheng, A. Bapna, O. Firat, D. Chen, M. X. Chen, H. Lee, J. Ngiam, Q. V. Le, Y. Wu, and Z. Chen, "Gpipe: Efficient training of giant neural networks using pipeline parallelism," in Advances in Neural Information Processing Systems 32: Annual Conference on Neural Information Processing Systems, 2019, pp. 103–112. [Online]. Available: https://proceedings.neurips.cc/paper/2019/hash/093f65e080a295f8076b1c5722a46aa2-Abstract.html
- [31] R. Ito, S. P. Liew, T. Takahashi, Y. Sasaki, and M. Onizuka, "Scaling private deep learning with low-rank and sparse gradients," ArXiv, vol. abs/2207.02699, 2022. [Online]. Available: https://api.semanticscholar. org/CorpusID:250311540
- [32] S. P. Karimireddy, Q. Rebjock, S. Stich, and M. Jaggi, "Error feedback fixes SignSGD and other gradient compression schemes," in *Proceedings of the 36th International Conference on Machine Learning*, ser. Proceedings of Machine Learning Research, vol. 97, 2019, pp. 3252–3261. [Online]. Available: https://proceedings.mlr.press/v97/karimireddy19a.html
- [33] V. Karpukhin, B. Oguz, S. Min, P. Lewis, L. Wu, S. Edunov, D. Chen, and W.-t. Yih, "Dense passage retrieval for open-domain question answering," in *Proceedings of the 2020 Conference on Empirical Methods in Natural Language Processing (EMNLP)*, 2020, pp. 6769–6781. [Online]. Available: https://aclanthology.org/2020.emnlpmain 550/
- [34] D. Lepikhin, H. Lee, Y. Xu, D. Chen, O. Firat, Y. Huang, M. Krikun, N. M. Shazeer, and Z. Chen, "Gshard: Scaling giant models with conditional computation and automatic sharding," ArXiv, vol. abs/2006.16668, 2020. [Online]. Available: https://api.semanticscholar. org/CorpusID:220265858
- [35] S. Li, Y. Zhao, R. Varma, O. Salpekar, P. Noordhuis, T. Li, A. Paszke, J. Smith, B. Vaughan, P. Damania, and S. Chintala, "Pytorch distributed: experiences on accelerating data parallel training," *Proc. VLDB Endow.*, vol. 13, no. 12, p. 3005–3018, 2020. [Online]. Available: https://doi.org/10.14778/3415478.3415530
- [36] S. Li, H. Liu, Z. Bian, J. Fang, H. Huang, Y. Liu, B. Wang, and Y. You, "Colossal-ai: A unified deep learning system for large-scale

- parallel training," in *Proceedings of the 52nd International Conference on Parallel Processing*, ser. ICPP '23, 2023, p. 766–775. [Online]. Available: https://doi.org/10.1145/3605573.3605613
- [37] S. Li, T. Ben-Nun, S. D. Girolamo, D. Alistarh, and T. Hoefler, "Taming unbalanced training workloads in deep learning with partial collective operations," in *Proceedings of the 25th ACM SIGPLAN Symposium on Principles and Practice of Parallel Programming*, ser. PPoPP '20, 2020, p. 45–61. [Online]. Available: https://doi.org/10.1145/3332466.3374528
- [38] S. Li and T. Hoefler, "Near-optimal sparse allreduce for distributed deep learning," in *Proceedings of the 27th ACM SIGPLAN Symposium* on *Principles and Practice of Parallel Programming*, ser. PPoPP '22, 2022, p. 135–149. [Online]. Available: https://doi.org/10.1145/3503221. 3508399
- [39] A. Liu, B. Feng, B. Xue, B. Wang, B. Wu, C. Lu, C. Zhao, C. Deng, C. Zhang, C. Ruan et al., "Deepseek-v3 technical report," arXiv preprint arXiv:2412.19437, 2024.
- [40] I. Loshchilov and F. Hutter, "SGDR: stochastic gradient descent with warm restarts," in 5th International Conference on Learning Representations (ICLR). OpenReview.net, 2017. [Online]. Available: https://openreview.net/forum?id=Skq89Scxx
- [41] T. Mihaylov, P. Clark, T. Khot, and A. Sabharwal, "Can a suit of armor conduct electricity? a new dataset for open book question answering," in *Proceedings of the 2018 Conference on Empirical Methods in Natural Language Processing*, 2018, pp. 2381–2391. [Online]. Available: https://aclanthology.org/D18-1260/
- [42] K. Mishchenko, F. Bach, M. Even, and B. Woodworth, "Asynchronous sgd beats minibatch sgd under arbitrary delays," in *Proceedings of* the 36th International Conference on Neural Information Processing Systems, ser. NIPS '22, 2022.
- [43] K. Nagrecha and A. Kumar, "Hydra: A system for large multi-model deep learning," ArXiv, vol. abs/2110.08633, 2021. [Online]. Available: https://api.semanticscholar.org/CorpusID:239017028
- [44] D. Narayanan, A. Harlap, A. Phanishayee, V. Seshadri, N. R. Devanur, G. R. Ganger, P. B. Gibbons, and M. Zaharia, "Pipedream: generalized pipeline parallelism for dnn training," in *Proceedings of the 27th ACM Symposium on Operating Systems Principles*, ser. SOSP '19, 2019, p. 1–15. [Online]. Available: https://doi.org/10.1145/3341301.3359646
- [45] D. Narayanan, A. Phanishayee, K. Shi, X. Chen, and M. Zaharia, "Memory-efficient pipeline-parallel dnn training," in *Proceedings of the* 38th International Conference on Machine Learning, ser. Proceedings of Machine Learning Research, vol. 139, 2021, pp. 7937–7947. [Online]. Available: https://proceedings.mlr.press/v139/narayanan21a.html
- [46] D. Narayanan, M. Shoeybi, J. Casper, P. LeGresley, M. Patwary, V. Korthikanti, D. Vainbrand, P. Kashinkunti, J. Bernauer, B. Catanzaro, A. Phanishayee, and M. Zaharia, "Efficient large-scale language model training on gpu clusters using megatron-lm," in *Proceedings of the International Conference for High Performance Computing, Networking, Storage and Analysis*, ser. SC '21, 2021, pp. 1–15. [Online]. Available: https://doi.org/10.1145/3458817.3476209
- [47] OpenAI, "GPT-4 technical report," CoRR, vol. abs/2303.08774, 2023.
  [Online]. Available: https://doi.org/10.48550/arXiv.2303.08774
- [48] D. A. Patterson, J. Gonzalez, Q. V. Le, C. Liang, L.-M. Munguía, D. Rothchild, D. R. So, M. Texier, and J. Dean, "Carbon emissions and large neural network training," ArXiv, vol. abs/2104.10350, 2021. [Online]. Available: https://api.semanticscholar.org/CorpusID: 233324338
- [49] PyTorch, "Accelerating PyTorch DDP by 10X With PowerSGD," https://medium.com/pytorch/accelerating-pytorch-ddp-by-10x-with-powersgd-585aef12881d, 2021, [Accessed 09-04-2025].
- [50] Z. Qu, S. Guo, H. Wang, B. Ye, Y. Wang, A. Y. Zomaya, and B. Tang, "Partial synchronization to accelerate federated learning over relayassisted edge networks," *IEEE Transactions on Mobile Computing*, vol. 21, no. 12, pp. 4502–4516, 2022.
- [51] A. Radford, J. Wu, R. Child, D. Luan, D. Amodei, I. Sutskever et al., "Language models are unsupervised multitask learners," *OpenAI blog*, vol. 1, no. 8, p. 9, 2019.
- [52] S. Rajbhandari, J. Rasley, O. Ruwase, and Y. He, "Zero: memory optimizations toward training trillion parameter models," in *Proceedings* of the International Conference for High Performance Computing, Networking, Storage and Analysis, ser. SC '20, 2020, pp. 1–16.
- [53] J. Rasley, S. Rajbhandari, O. Ruwase, and Y. He, "Deepspeed: System optimizations enable training deep learning models with over 100 billion parameters," in *Proceedings of the 26th ACM SIGKDD International Conference on Knowledge Discovery &*

- *Data Mining*, 2020, p. 3505–3506. [Online]. Available: https://doi.org/10.1145/3394486.3406703
- [54] M. Reid, N. Savinov, D. Teplyashin, D. Lepikhin, T. P. Lillicrap et al., "Gemini 1.5: Unlocking multimodal understanding across millions of tokens of context," ArXiv, vol. abs/2403.05530, 2024. [Online]. Available: https://api.semanticscholar.org/CorpusID:268297180
- [55] K. Sakaguchi, R. L. Bras, C. Bhagavatula, and Y. Choi, "Winogrande: an adversarial winograd schema challenge at scale," *Commun. ACM*, vol. 64, no. 9, p. 99–106, 2021. [Online]. Available: https://doi.org/10.1145/3474381
- [56] F. Seide, H. Fu, J. Droppo, G. Li, and D. Yu, "1-bit stochastic gradient descent and its application to data-parallel distributed training of speech dnns," in 15th Annual Conference of the International Speech Communication Association, 2014, pp. 1058–1062. [Online]. Available: https://doi.org/10.21437/Interspeech.2014-274
- [57] S. Shen, L. Hou, Y. Zhou, N. Du, S. Longpre, J. Wei, H. W. Chung, B. Zoph, W. Fedus, X. Chen, T. Vu, Y. Wu, W. Chen, A. Webson, Y. Li, V. Y. Zhao, H. Yu, K. Keutzer, T. Darrell, and D. Zhou, "Mixture-of-experts meets instruction tuning: A winning combination for large language models," in *The Twelfth International Conference on Learning Representations (ICLR)*, 2024. [Online]. Available: https://openreview.net/forum?id=6mLjDwYte5
- [58] S. Shi, X. Chu, K. C. Cheung, and S. See, "Understanding top-k sparsification in distributed deep learning," ArXiv, vol. abs/1911.08772, 2019. [Online]. Available: https://api.semanticscholar.org/CorpusID: 208175673
- [59] S. Shi, X. Chu, and B. Li, "Exploiting simultaneous communications to accelerate data parallel distributed deep learning," in *IEEE INFOCOM* 2021 - IEEE Conference on Computer Communications, 2021, pp. 1–10.
- [60] S. Shi, X. Chu, and B. Li, "Mg-wfbp: Merging gradients wisely for efficient communication in distributed deep learning," *IEEE Transactions on Parallel and Distributed Systems*, vol. 32, no. 8, pp. 1903–1917, 2021.
- [61] M. Shoeybi, M. Patwary, R. Puri, P. LeGresley, J. Casper, and B. Catanzaro, "Megatron-lm: Training multi-billion parameter language models using model parallelism," *ArXiv*, vol. abs/1909.08053, 2019. [Online]. Available: https://api.semanticscholar.org/CorpusID: 202660670
- [62] J. Song, J. Yim, J. Jung, H. Jang, H.-J. Kim, Y. Kim, and J. Lee, "Optimus-cc: Efficient large nlp model training with 3d parallelism aware communication compression," in *Proceedings of* the 28th ACM International Conference on Architectural Support for Programming Languages and Operating Systems, Volume 2, ser. ASPLOS 2023, 2023, p. 560–573. [Online]. Available: https: //doi.org/10.1145/3575693.3575712
- [63] S. U. Stich, J.-B. Cordonnier, and M. Jaggi, "Sparsified sgd with memory," in *Proceedings of the 32nd International Conference on Neural Information Processing Systems*, ser. NIPS'18, 2018, p. 4452–4463.
- [64] H. Tang, S. Gan, A. A. Awan, S. Rajbhandari, C. Li, X. Lian, J. Liu, C. Zhang, and Y. He, "1-bit adam: Communication efficient large-scale training with adam's convergence speed," in *Proceedings of the 38th International Conference on Machine Learning (ICML)*, vol. 139, 2021, pp. 10118–10129. [Online]. Available: http://proceedings.mlr.press/v139/tang21a.html
- [65] Z. Tang, S. Shi, X. Chu, W. Wang, and B. Li, "Communication-efficient distributed deep learning: A comprehensive survey," ArXiv, vol. abs/2003.06307, 2020. [Online]. Available: https://api.semanticscholar. org/CorpusID:212718058
- [66] T. Vogels, S. P. Karimireddy, and M. Jaggi, "Powersgd: Practical low-rank gradient compression for distributed optimization," in Advances in Neural Information Processing Systems, 2019, pp. 14236– 14245. [Online]. Available: https://proceedings.neurips.cc/paper/2019/ hash/d9fbed9da256e344c1fa46bb46c34c5f-Abstract.html
- [67] T. Vogels, S. P. Karimireddy, and M. Jaggi, "Practical low-rank communication compression in decentralized deep learning," in *Proceedings of the 34th International Conference on Neural Information Processing Systems*, ser. NIPS '20, 2020, pp. 14171–14181.
- [68] B. Wang, Q. Xu, Z. Bian, and Y. You, "2.5-dimensional distributed model training," *ArXiv*, vol. abs/2105.14500, 2021. [Online]. Available: https://api.semanticscholar.org/CorpusID:235254533
- [69] S. Wang, A. Pi, X. Zhou, J. Wang, and C. Xu, "Overlapping communication with computation in parameter server for scalable DL training," *IEEE Trans. Parallel Distributed Syst.*, vol. 32, no. 9, pp.

- 2144–2159, 2021. [Online]. Available: https://doi.org/10.1109/TPDS. 2021.3062721
- [70] J. Wangni, J. Wang, J. Liu, and T. Zhang, "Gradient sparsification for communication-efficient distributed optimization," in *Proceedings of* the 32nd International Conference on Neural Information Processing Systems, ser. NIPS'18, 2018, p. 1306–1316.
- [71] Q. Xu and Y. You, "An efficient 2d method for training super-large deep learning models," in 2023 IEEE International Parallel and Distributed Processing Symposium (IPDPS), 2023, pp. 222–232.
- [72] Y. Yoshida and T. Miyato, "Spectral norm regularization for improving the generalizability of deep learning," *ArXiv*, vol. abs/1705.10941, 2017. [Online]. Available: https://api.semanticscholar.org/CorpusID:19183245
- [73] A. Yurtsever, M. Udell, J. Tropp, and V. Cevher, "Sketchy Decisions: Convex Low-Rank Matrix Optimization with Optimal Storage," in *Proceedings of the 20th International Conference on Artificial Intelligence and Statistics*, ser. Proceedings of Machine Learning Research, vol. 54, 2017, pp. 1188–1196. [Online]. Available: https://proceedings.mlr.press/v54/yurtsever17a.html
- [74] R. Zellers, A. Holtzman, Y. Bisk, A. Farhadi, and Y. Choi, "HellaSwag: Can a machine really finish your sentence?" in *Proceedings of the 57th Annual Meeting of the Association for Computational Linguistics*, 2019, pp. 4791–4800. [Online]. Available: https://aclanthology.org/P19-1472/
- [75] C. Zhang, H. Tian, W. Wang, and F. Yan, "Stay fresh: Speculative synchronization for fast distributed machine learning," in 2018 IEEE 38th International Conference on Distributed Computing Systems (ICDCS), 2018, pp. 99–109.
- [76] H. Zhang, Z. Zheng, S. Xu, W. Dai, Q. Ho, X. Liang, Z. Hu, J. Wei, P. Xie, and E. P. Xing, "Poseidon: An efficient communication architecture for distributed deep learning on GPU clusters," in *Proceedings of the 2017 USENIX Annual Technical Conference*, 2017, pp. 181–193. [Online]. Available: https://www.usenix.org/conference/atc17/technical-sessions/presentation/zhang
- [77] K. Zhao, S. Huang, P. Pan, Y. Li, Y. Zhang, Z. Gu, and Y. Xu, "Distribution adaptive INT8 quantization for training cnns," in *Thirty-Fifth AAAI Conference on Artificial Intelligence (AAAI)*, 2021, pp. 3483–3491. [Online]. Available: https://doi.org/10.1609/aaai.v35i4.16462